

# **An updated electromagnetic simulation of the HERA antenna with CST and comparison with measurements**

Nicolas Fagnoni, Eloy De Lera Acedo  
Department of Physics, University of Cambridge, UK

10<sup>th</sup> December 2016

## **Abstract**

This memo presents an improved model of the HERA antenna as well as the parameters used to simulate its electromagnetic properties. The antenna consists of a faceted parabolic reflector with a diameter of 14 m, a PAPER feed made up of two perpendicular dipoles between two metal plates, and a cylindrical cage above the feed. Based on the work of optimisation performed by David DeBoer <sup>1</sup>, the antenna is thoroughly modelled with CST, and the effects of the different materials are also taken into account. In our simulation, a dipole is excited via a differential termination port with a 100- $\Omega$  impedance, by a Gaussian pulse centred on 150 MHz and with a bandwidth of 200 MHz. The transient solver of CST is used to characterise the antenna in the time domain, and in particular the scattering parameters of the antenna are computed between 50 and 250 MHz. Then, these results are compared to the S-parameters measured on a real HERA antenna built in Cambridge (UK) at Lord's Bridge, by using a 2-port VNA connected to the bars of a dipole via 2 50- $\Omega$  coaxial cables. The S-parameters obtained with our simulation and measurements do agree well. Thus, the goal of this document is to clearly describe this model, which can be used to accurately study the properties of the antenna and its effects on the received signal. Lastly, the results of our simulations can be found in the following GitHub repository: <https://github.com/Nicolas-Fagnoni/Simulations>.

## **1. Introduction**

While the first antennas of HERA are being built in the Karoo desert in South Africa, it is still necessary to precisely assess the performance of the dish, as well as to carefully model the chromatic effects caused by the additional reflections which occur between the feed and the reflector, and between the structure of the adjacent antennas (mutual coupling). Indeed, these chromatic effects can significantly affect the characterisation of the EoR delay power spectrum by spreading the foreground signal into the delay domain. Thus, it is essential to correctly understand the interactions between the received signal and the dish, by simulating and analysing the antenna response <sup>2 3 4 5</sup>. Furthermore, electromagnetic simulations can also be used to analyse the effects of inaccuracies in the construction of the antennas, for instance a variation in the position of the feed. Lastly, a new feed is currently being developed with the objective to characterise the EoR signal with a wider bandwidth between 50 and 250 MHz, and two different designs are going to be tested: one using a Vivaldi feed (University of Cambridge), and the other one a sinuous feed (MIT). Therefore, in order to have coherent results between the different teams working on HERA and make fair comparisons, it is preferable to use a common and reliable electromagnetic model. Indeed, small modifications in the model may noticeably change the simulation results, such as the radiation pattern or the antenna response. The purpose of this memo is to present a simulation of the antenna using CST and validated by measurements performed on a real HERA dish. Indeed, the University of Cambridge has built 3 new HERA antennas, complying with the design of the antennas present in South Africa.

## 2. CST simulation

### 2.1. Antenna model

Our CST model can be divided into 3 main elements: the reflector, the feed, and a cylindrical cage located just above the feed (see *Figure 1*).

The reflector is modelled by a faceted paraboloid made up of 24 segments in aluminium, and has a diameter of 14 m, a focal ratio of 0.32, and is about 2.7-m high. At its vertex, a cylindrical concrete slab with a 91-cm diameter, called the “hub”, firmly holds the PVC pipes supporting the structure of the antenna. This hub has also a 46-cm diameter hole at its centre crossed by 2 perpendicular PVC tubes. The presence of a vertical metal rod used to tie the bottom of the feed to the vertex is also included. Besides, the effect of the soil underneath is also considered by adding a layer of dielectric material. It is important to carefully model the centre of the antenna, since this zone plays a significant role in the reflections of the signal with the feed. Indeed, the concrete and the soil present at the vertex, absorb a part of the electromagnetic waves, which degrades the antenna aperture efficiency, but also reduces the amplitude of the additional reflections between the feed and the parabola.

The PAPER feed consists of two perpendicular 1.3-m long dipoles made of copper, and measure the linear horizontal and vertical polarisations of the signal. Moreover, in order to broaden its frequency response, two aluminium discs are added, one below the dipoles, and one above. The extremities of the dipoles are ended by copper connectors, which are directly connected to the front-end electronics. The presence of the balun structure is also modelled by a brass tube terminated by two output coaxial cables, one for each polarity. The plastic structure which supports the dipoles and the cylindrical cage has also been included in our simulation.

The feed of HERA is surrounded by a cylindrical structure which protects it from external reflections coming from adjacent antennas, which are only separated by 60 cm. This structure is made up of two elements in aluminium in contact: the “backplane”, which is a 172-cm diameter disc, and a cylindrical “skirt” with a height of 36 cm. The cylindrical structure is suspended by 3 ropes, 4.9 m above the dish, but this height can be adjusted.

Lastly, our simulation does also take into account the electrical and electromagnetic properties of the different materials, by using the material library of CST. Thus, electric conductors have a finite conductivity  $\sigma$  which implies a certain resistivity, and so some conduction losses caused by the metal elements. Moreover, the effects of the dielectrics on the propagation and attenuation of the electromagnetic wave is characterised by their complex permittivity  $\epsilon$ . In particular, the dielectric losses are quantified by the “loss tangent”  $\tan \delta$ . As a reminder, the permittivity  $\epsilon$  is a complex number,  $\epsilon = \epsilon' - i\epsilon''$ , defined by its real part  $\epsilon' = \epsilon_0 \epsilon_r$  with  $\epsilon_0$  the vacuum permittivity and  $\epsilon_r$  the relative permittivity of the material, and by its imaginary part  $\epsilon''$  which is related to the attenuation of the wave. Thus the “loss tangent”  $\tan \delta$  at the angular frequency  $\omega$  is defined by <sup>6</sup>:

$$\tan \delta = \frac{\omega \epsilon'' + \sigma}{\omega \epsilon'} \quad (1)$$

Conduction and dielectric losses directly affect the “radiation efficiency” and so the gain of the antenna.

The dimensions of the main elements as well as the characteristics of the material used, are summarised at the end of this document.

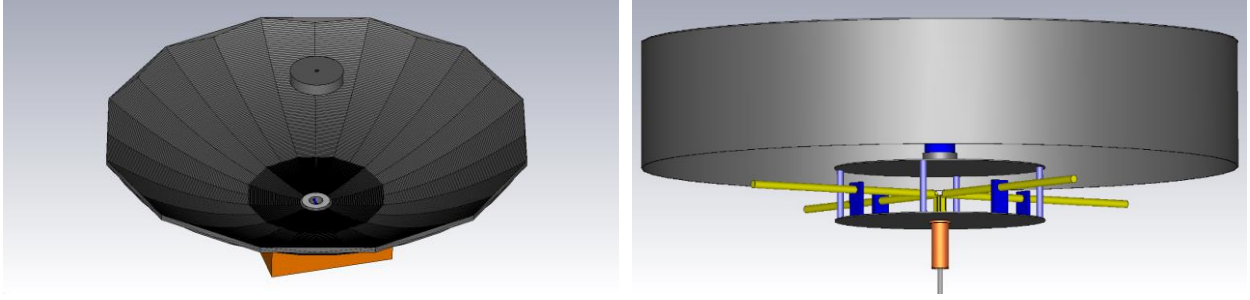


Figure 1. CST simulation model of the HERA dish and feed.

## 2.2. Simulation parameters

The study of the antenna response and its electromagnetic properties is performed by using the time domain solver of CST. This “transient solver” is based on the “Finite Integration Technique”, which divides the delimited space into adjacent hexahedral cells, and then tries to solve the discretised Maxwell’s equations in their integral form on the facets of each cell, guaranteeing the consistency of the solutions between each cell. This solver is very stable and efficient for problems with a complex geometry, and is also particularly suitable for high frequency simulation and wide band analysis. Indeed, it can characterise the system in the time domain as well as in the frequency domain with only one calculation run, unlike frequency solvers.

Concerning the presented results, we used a broadband Gaussian pulse centred on 150 MHz with a bandwidth of 200 MHz as excitation signal, in order to simulate the antenna characteristics between 50 and 250 MHz. Lasting about 25 ns, this signal can either excite an external plane wave or a discrete termination port. Discrete termination ports are a simplified representation of the feed line, which connect two points of the antenna structure, and can deliver or absorb power. They are equivalent to a current source with an internal impedance, which should in theory represent the impedance of the RF front-end, or the VNA in the case of our measurements. Thus, by exciting a termination port, it is possible to directly compute the radiation pattern of the antenna, its impedance and the S-parameters. On the other hand, the excitation of the antenna by a plane wave allows us to characterise the antenna response when receiving a signal. This will be the subject of a next memo, emphasising the effects of a realistic impedance termination on the characteristics of the antenna.

It is also important to underline that in our simulation a termination port links the 2 arms of a dipole together (see Figure 2). Indeed, a dipole is designed to work with a balanced line at its input, and so to produce or response to a differential signal. Thus for a given dipole, both arms are simultaneously excited by the same signal coming from the “differential” port, but phase shifted by 180°. This approach is called “mixed mode” and allows us to directly simulate the differential S-parameters and impedance of the antenna for a given dipole. However, it is technically not possible to simultaneously excite both ports with a differential signal with our own VNA, unless we use a balun which then will have to be de-embedded from our measurements. In the case of our measurements, each dipole bar is independently excited by one of the ports of the VNA. This “single-ended mode” configuration is equivalent to measure the S-parameters of a 2-port system for a single dipole. Nevertheless, the differential S-parameters can be deduced from the S-parameters measured in this configuration without balun, on condition that there is no coupling between the feed lines of the ports, which is generally the case since the coaxial cables used are shielded. In particular, the differential S11-parameter for a dipole is given by <sup>78</sup>:

$$S_{d11} = \frac{S_{11} - S_{12} - S_{21} + S_{22}}{2} \quad (2)$$

Lastly, since the 2 ports of our VNA have an impedance of  $50\ \Omega$ , the differential impedance of the termination port used in our simulation must be set to  $50 + 50 = 100\ \Omega$ .

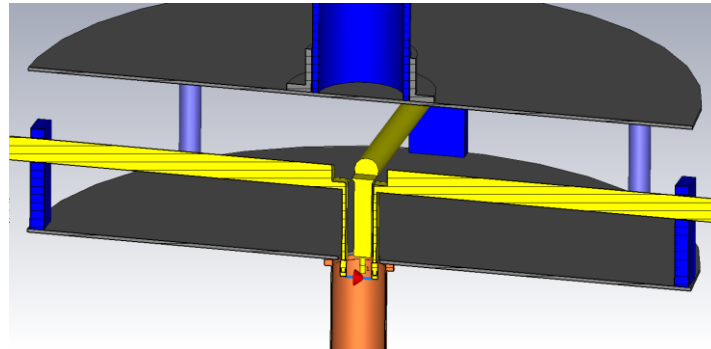


*Figure 2. Differential termination port (in red) with an impedance of  $100\ \Omega$  and linking the 2 bars of a dipole.*

Except the model itself, there are two other main elements which strongly affect the results of our simulation: the simulation time and the mesh. The simulation time is directly related to the amplitude of the time signal and the total energy inside the calculation domain: when the latter is below a certain threshold, the simulation stops. Then, the frequency results, such as the S-parameters, are obtained by Fourier transforming the time results. The longer the simulation time is, the more accurate the S-parameters are, since a greater number of additional reflections are taken into account for the calculations. The presented results are obtained with a simulation time of 200 ns and a time step of 0.003 ns, which is equivalent to an accuracy of about -40 dB. It is sufficient for a good characterisation of the S-parameters which agrees with our measurements. However, for a very accurate time domain simulation and in order to measure the amplitude of the additional reflections below -60 dB, we would recommend to manually set the simulation time to 500 ns.

The background is defined as vacuum with open boundaries for propagation in free space, and the simulation volume is delimited by a region of 15.0 m x 15.0 m x 7.1 m. The generation of the mesh must be carefully performed, since the results are very sensitive to this parameter. In particular, the antenna contains large and small elements which have to be properly delimited by the mesh, in order to avoid spaced elements from being “in contact”. Thus, in our detailed model, the simulation volume is divided into 47 million hexahedral cells, and the mesh around the smallest structures, in particular in the feed, is controlled by locally increasing the density of cells. With these parameters, it takes about 5 hours to run this simulation, using 2 CPU cores with a total of 16 parallel threads at 2.6 GHz, 29 GB of RAM, and without GPU acceleration. The number of cells are relatively high in this simulation in order to have accurate results which can be used as reference. However, during the optimisation process when different models are tested, we suggest to use first a simpler model. For example, a “simplified” version with 12.1 million cells, “perfect electric conductors” (PEC) and lossless materials can be simulated in 45 min. The goal of these adjustments is to find a good balance between accuracy and computation time. The S11-parameter from these 2 simulations are given in *Figure 9* for comparison.

## 3. Measurements

### 3.1. Feed only

#### 3.1.1. Measurement environment

First, we measured the S-parameters of the feed only with a VNA. In order to make the measurements easier, the feed was positioned upside-down on the ground, and in a remote area to avoid any significant interferences and reflections. On site, the ground is actually a copper grid which can be seen as a circular ground plane, with a concrete slab underneath (see *Figure 3*). This grid has a diameter of 15 m and a 30-cm meshing. The 2 50- $\Omega$  ports of the VNA were connected to the ports of a dipole via LBC 240 coaxial cables with a length of 35 m. The effects of the cables on the S-parameter measurements were also calibrated and automatically compensated by the device. Lastly, because the dipole bars are terminated by pin connectors, we had to insert a small “adapter board” to connect them to the SMA measurement cables (see *Figure 4*). Moreover, when the S-parameters of a dipole were measured, the connectors of the other dipole were terminated by 50- $\Omega$  SMA terminations.

Then, in order to make a fair comparison, we also modified our simulation to take into account the effects of the measurement environment. First, we modelled the metal grid by a simple circular ground plane and simulated the presence of the cables. This model is divided into 13.9 million cells and uses a simulation time of 80 ns. We also tried a more “sophisticated” model with a realistic metal grid and the concrete slab (see *Figure 5*). However, this second model requires more than 42 million cells to work.



*Figure 3. HERA feed and S-parameter measurements at Lord's Bridge (Cambridge).*

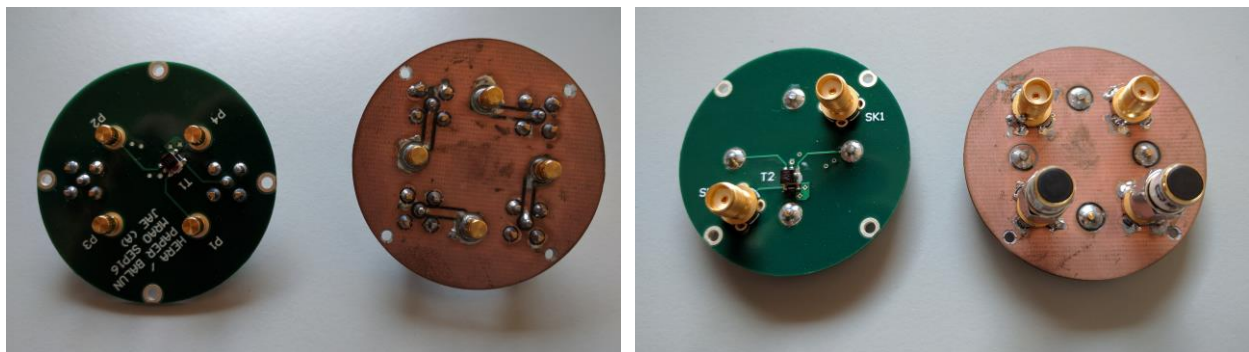


*Figure 4. Adapter board used to connect the pin connectors of the dipole bars to the measurement SMA cables.*

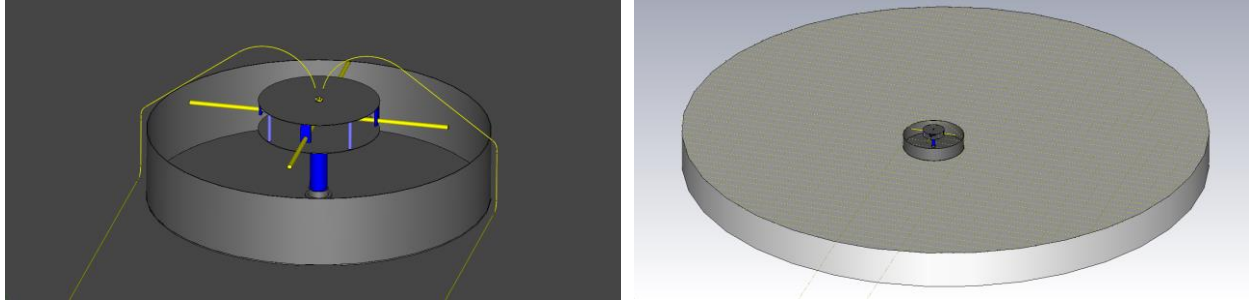


Figure 5. CST simulation of the feed, taking into account the effects of the measurement environment (measurement cables, metal grid and concrete soil).

### 3.1.2 Results

Figure 6 below shows the measured and simulated S-parameters (model with circular ground plane); as we can see these results do agree well. Two configurations were considered: one in which the measurement cables were along the excited dipole, and the other one in which they are perpendicular, and indeed we can notice that the presence of the cables do slightly modify the measured S-parameters. Parallel to the dipole, the metal shield of the cables interacts by absorbing and re-radiating a part of the electromagnetic wave coming from the dipole, which increases the reflection coefficient. On the other hand, when the cables are perpendicular to the excited dipole, their presence does not really affect the S-parameters, since the simulations show almost similar results when there is no cable. In addition, we ran the simulation with the realistic metal grid and concrete slab, and the results are equivalent: even though the meshing is relatively large (30 cm) with respect to the wavelengths (1.2 m – 6 m), the electromagnetic wave mainly “sees” the metal grid, which can be approximated by a circular ground plane.

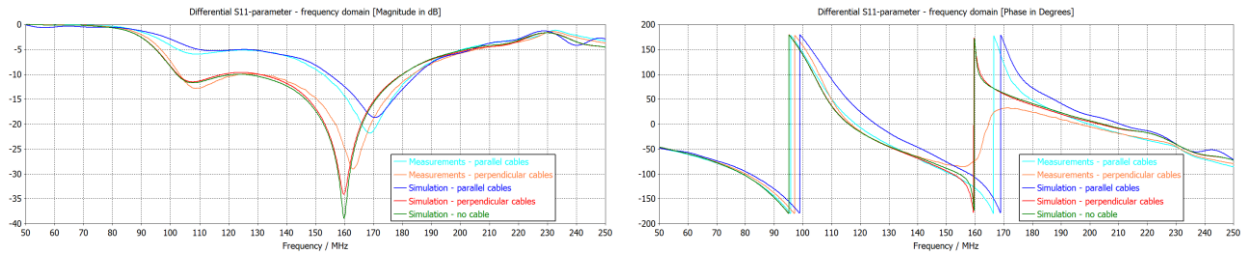
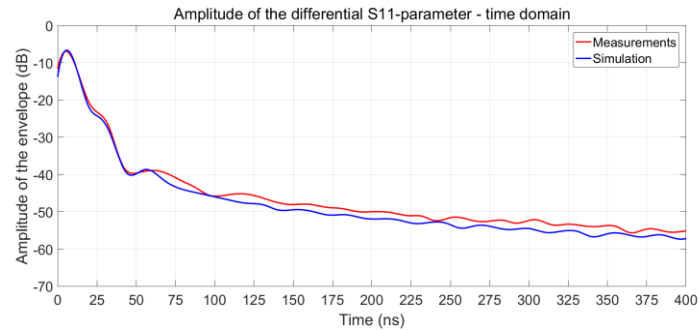


Figure 6. Differential S11-parameter of the feed in the frequency domain, from measurements and simulations (model with circular ground plane).

Furthermore, in order to quantify the amplitude of the reflections occurring at the interface between the feed and the front-end in the time domain, the inverse Fourier transform of the S11-parameter from 0 to 250 MHz is computed (see Figure 7); the results are displayed in dB scale by taking “ $20 \cdot \log_{10}$ ” of the absolute value of the linear amplitude. We can see that the reflections, mainly occurring within the cylindrical cage, quickly decay.





*Figure 7. Amplitude of the differential S11-parameter of the feed in the time domain, from measurements and simulation (configuration with perpendicular cables).*

## 3.2. HERA antenna

### 3.2.1. Measurement environment

After having obtained satisfactory results with the feed, we measured the S-parameters of the dish. The VNA is connected to a dipole in the same way as previously, and the feed is hung up at 4.9 m above the vertex (distance from the backplane to the ground). This time, the metal structure of the balun was screwed to the feed to account for its electromagnetic effects, but without the RF electronics inside. The antennas were also built in a remote environment, and in order to more accurately represent the effects of the soil that day (wet and loamy), we modified its dielectric properties ( $\epsilon_r$ : 19.89,  $\tan \delta$ : 0.03 at 150 MHz). We can see in *Figure 8* some pictures of the antennas built at Lord's Bridge and the CAD building plan designed with Autodesk Inventor (to be compared with our CST model in *Figure 1*).



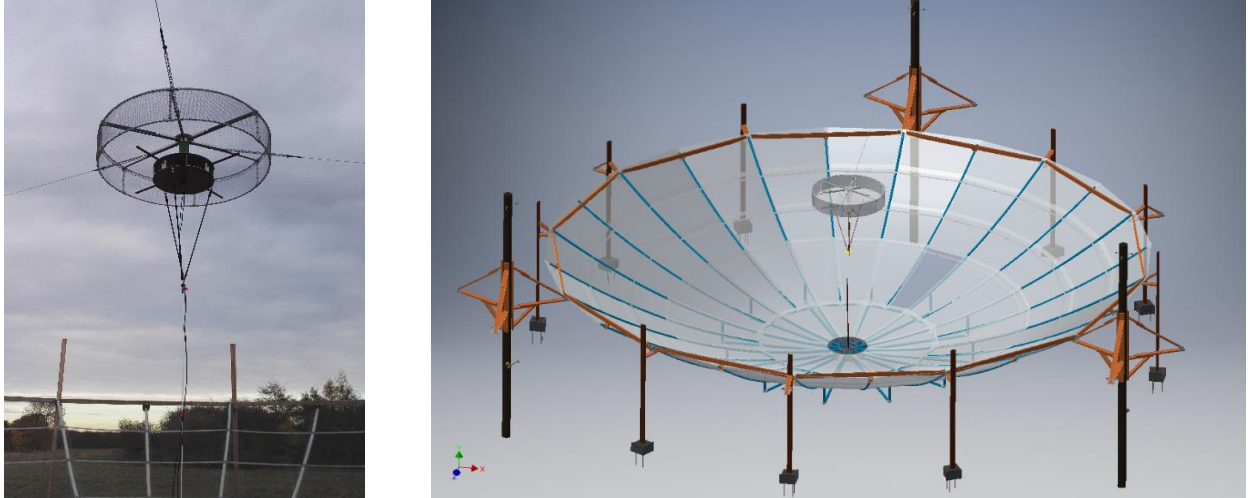


Figure 8. HERA antennas at Lord's Bridge and CAD building plan.

### 3.2.2 Results

As previously, we focus our analysis on the S-parameters. Even though the model is more complex with the addition of the parabola, our simulation and measurements still do agree rather well. It is also interesting to notice the effect of the number of cells on the results of the simulation: the “simplified” model with 12.1 million cells in the mesh, lossless materials and PEC metals, still gives coherent results, but obviously not as accurate as the simulation with 47 million cells. In order to check that this difference is mainly due to the number of cells, we also ran the same simplified simulation but using real materials this time, and we obtained nearly identical results. Furthermore, if we continue decreasing the number of cells, the results quickly deteriorate, and for example the two humps at 148 MHz and 169 MHz are not distinguishable anymore. Concerning the time-domain representation of the S11-parameter (see Figure 10), we can clearly notice the presence of multiple reflections occurring about every 33 ns, which corresponds to the round-trip time between the feed and the dish.

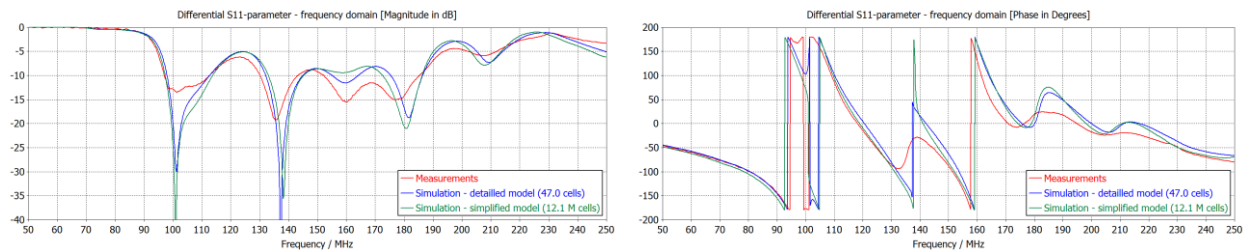


Figure 9. Differential S11-parameter of the antenna in the frequency domain, from measurements and simulation (with 47 and 12.1 million cells).



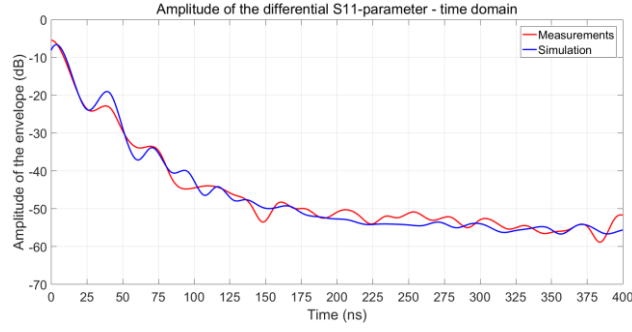


Figure 10. Amplitude of the differential  $S_{11}$ -parameter of the antenna in the time domain, from measurements and simulation (detailed model).

For information purpose, the antenna impedance, antenna efficiency, and directivity patterns every 20 MHz from our detailed simulation are given below. Indeed, these are essential parameters to describe the properties of the antenna, and they do not depend on the impedance termination. In particular, we can notice that the antenna impedance significantly varies across the frequency, which makes the impedance matching with the RF front-end difficult, even between 100 and 200 MHz, the current operating frequency band of HERA. As a consequence, a part of the incoming signal is reflected back at the interface between the dipoles and the RF-front end. Besides, since our simulation gives reliable results for the S-parameters, we can assume that the radiation patterns are also rather accurate, but this will need to be confirmed by proper beam measurements, using a drone for example<sup>9</sup>. Lastly, we can see that the radiation efficiency, which (only) accounts for dielectric and conduction losses within the antenna, is above 90% after 70 MHz, which means that the directivity and the gain of the antenna are almost identical. Thus, it is coherent to simplify the model by considering PEC for the metals and by neglecting the dielectric losses, in order to speed up the computation time.

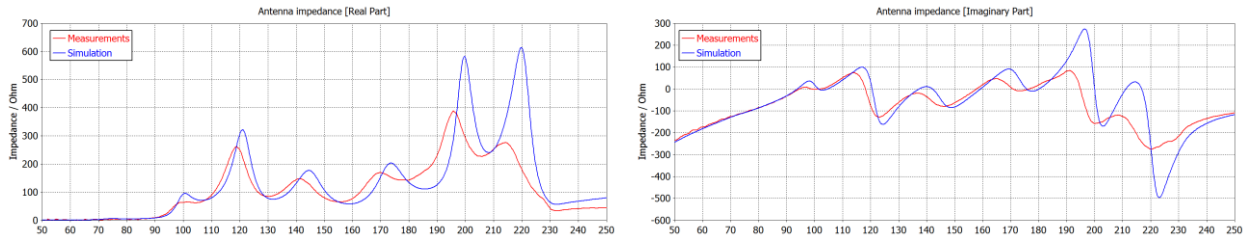


Figure 11. Real and imaginary part of the antenna impedance, from measurements and simulation.

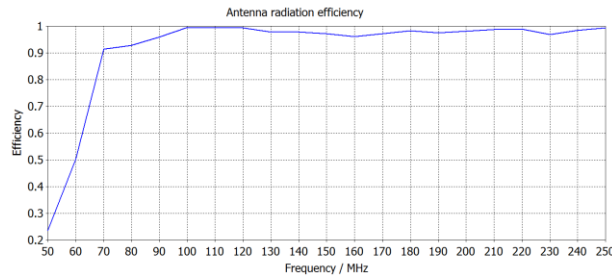


Figure 12. Radiation efficiency of the antenna, from simulation. It only accounts for the dielectric and conductivity losses within the antenna.

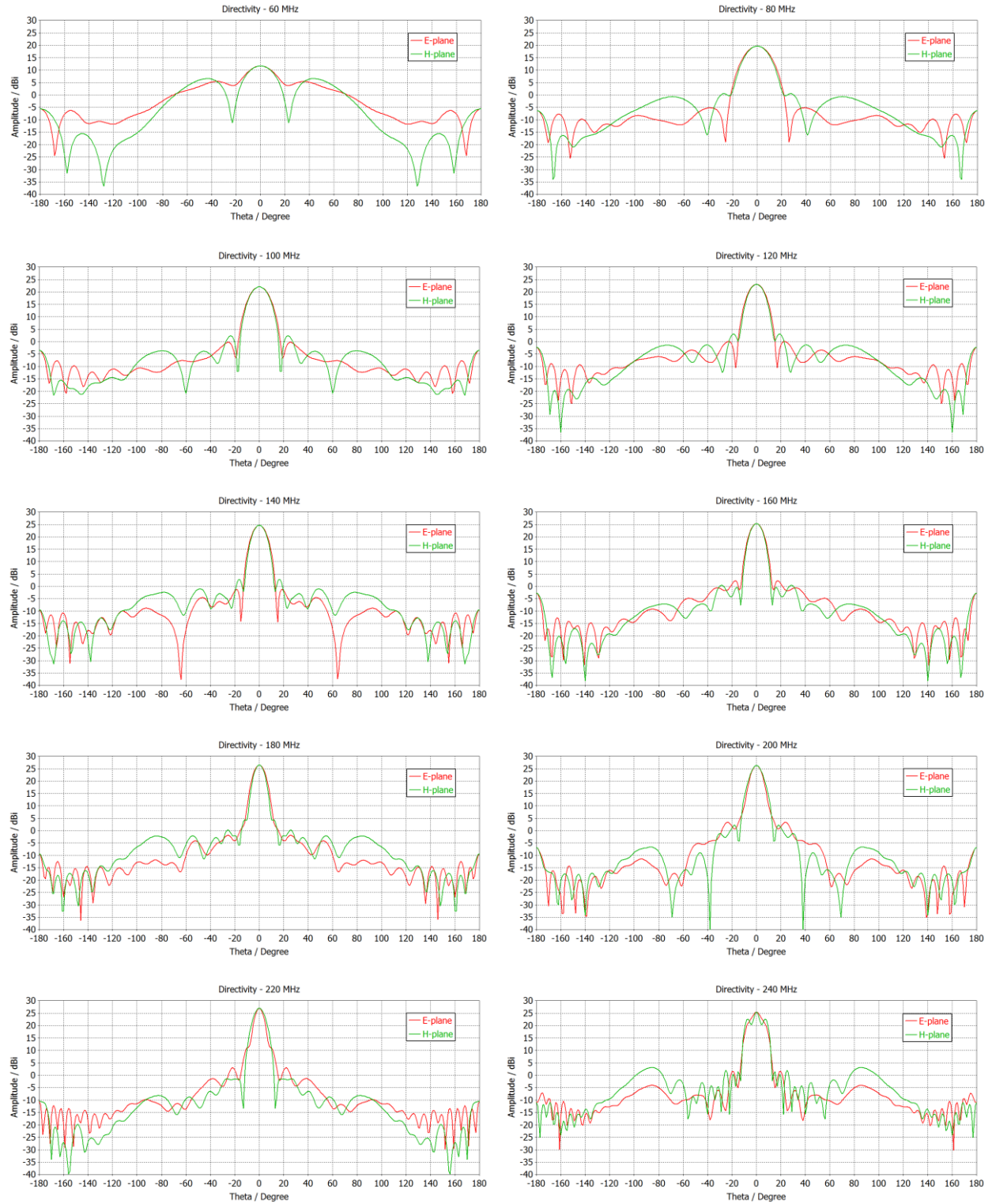


Figure 13. Cuts of the directivity pattern through the “E-plane” (red) and “H-plane” (green), every 20 MHz between 60 and 240 MHz. It does not account for any losses.

## 4. Conclusion

In this memo, we presented a reliable electromagnetic simulation of the HERA dish performed with CST, by thoroughly modelling the antenna and taking into account the effects of the materials. Furthermore, we measured the S-parameters of a real antenna built at Lord's Bridge with a VNA. For the moment, the effects of the RF front-end are not included in our simulation and measurements: the bars of a dipole were directly connected to the VNA by 2 50- $\Omega$  coaxial cables. The results from our simulation and measurements does agree well. Thus, we now have a reference model which can be used to correctly assess the performance of the antenna, investigate the chromatic effects induced by the dish on the received signal, improve the design, and compare results. The S-parameters, antenna impedance, and radiation beam pattern are available in GitHub: <https://github.com/Nicolas-Fagnoni/Simulations>. Lastly, in our next memo, we will present a new electromagnetic and electrical co-simulation which includes the effect of the RF-front and transmission cables on the time signal and antenna sensitivity. As we will see, it is important to properly model the antenna termination to characterise the additional reflections between the parabola and the feed.

## Appendix

Elements	Main dimensions	Material	Comments
<b>Parabola</b>	Diameter: 14 m Height: 2.7 m Focal ratio: 0.32	Aluminium	-Faceted (24 panels)
<b>Cylindrical hub</b>	Hub diameter: 91.4 cm Central hole diameter: 45.7 m  Metal rod height: 17.8 cm Metal rod diameter: 2.0 cm  PVC pipe 1 diameter: 6.3 cm PVC pipe 2 diameter: 9.0 cm	Concrete	-2 metal cylinders, one inside the hub and one outside, are present to reinforce its structure. - A vertical metal rod is present at the centre, as well as 2 perpendicular PVC pipes passing through the hub.
<b>Soil</b>	Length: 2 m Width: 2 m Thickness: 1 m	Dry sandy soil	-Must be extended to simulate the coupling between adjacent antennas. -Wet loamy soil for Cambridge.
<b>Dipoles</b>	Bar length: 65 cm Bar diameter: 2.2 cm Distance between bars: 2.5 cm Dipole length: 132.5 cm Feed element length: 7.3 cm	Copper	
<b>Plates</b>	Diameter: 61 cm Distance between plates: 14.9 cm	Aluminium	
<b>Dipole supports</b>	Length: 5.1 cm Width: 1.3 cm Height: 9.5 cm	PVC	
<b>Plate supports</b>	Diameter: 2.0 cm Height: 14.9 cm	Teflon	
<b>Top plate - cylindrical cage tube</b>	Diameter: 9.0 cm Height: 36.0 cm	PVC	
<b>Metal collars</b>	Diameter 1: 10.0 cm Diameter 2: 13.5 cm Total height: 4.4 cm	Aluminium	-Attach the tube to the top plate and cylindrical cage
<b>Cylindrical cage</b>	Diameter: 172.0 cm Skirt height: 36.0 cm Distance between the backplane and the ground: 4.9 m	Aluminium	-Skirt and backplane in contact
<b>Balun</b>	Diameter 1: 6.4 cm Diameter 2: 5.1 cm Total height: 13.7 cm	Brass	
<b>RG6 coaxial cables</b>	Conductor diameter: 0.5 cm Length: 3.9 m	Aluminium	
<b>Feed bar – balun connectors</b>	Diameter: 0.56 cm Height: 1.5 cm	Copper	

Table 1. Dimensions of the main elements in the CST simulation.

Material	Electromagnetic properties
Aluminium	$\sigma: 3.56 \cdot 10^7 \text{ S/m}$
Copper	$\sigma: 5.8 \cdot 10^7 \text{ S/m}$
Brass (65% copper, 35% zinc)	$\sigma: 1.59 \cdot 10^7 \text{ S/m}$
PVC	$\epsilon_r: 4.00$ $\tan \delta: 6 \cdot 10^{-2}$
Teflon	$\epsilon_r: 2.10$ $\tan \delta: 6 \cdot 10^{-6}$
Sandy dry soil	$\epsilon_r: 2.55$ $\tan \delta: 1 \cdot 10^{-3}$
Concrete	$\epsilon_r: 5.90$ $\tan \delta: 2 \cdot 10^{-2}$

Table 2. electromagnetic properties of the materials used in our CST simulation at 150 MHz.

## References

- <sup>1</sup> DeBoer, D. HERA Phase I Feed Design. (2015) Available at: <http://reionization.org/wp-content/uploads/2015/01/feedP1.pdf>
- <sup>2</sup> Neben, A. R., *et al.* The Hydrogen Epoch of Reionization Array Dish I: beam pattern measurements and science implications. (2016)
- <sup>3</sup> Ewall-Wice, A. *et al.* The Hydrogen Epoch of Reionization Array Dish II: characterization of spectral struture with electromagnetic simulations and its science implications. (2016)
- <sup>4</sup> Nipanjana, P. *et al.* The Hydrogen Epoch of Reionization Array Dish III: measuring chromaticity of prototype element with reflectometry. (2016)
- <sup>5</sup> Thyagarajan, N., *et al.* Effects of antenna beam chromaticity on redshifted 21 cm power spectrum and implications for Hydrogen Epoch of Reionization Array. (2016)
- <sup>6</sup> Pozar, D. in *Microwave Engineering* (ed. Wiley) 9–11. (1998)
- <sup>7</sup> Huynh, A., Karlsson, M. & Gong, S. in *Advanced Microwave Circuits and Systems* (ed. Zhurbenko, V.). (2010) Available at: [http://www.intechopen.com/source/pdfs/9636/InTech-Mixed\\_mode\\_s\\_parameters\\_and\\_conversion\\_techniques.pdf](http://www.intechopen.com/source/pdfs/9636/InTech-Mixed_mode_s_parameters_and_conversion_techniques.pdf)
- <sup>8</sup> Maxim Integrated Product. Single-Ended and Differential S-Parameters. (2008) Available at: [notes-application.abcelectronique.com/003/3-5169.pdf](http://notes-application.abcelectronique.com/003/3-5169.pdf)
- <sup>9</sup> Jacobs, D. C., *et al.* The external calibrator for hydrogen observatories. (2016)